Research Square

Preprints are preliminary reports that have not undergone peer review.
They should not be considered conclusive, used to inform clinical practice,
or referenced by the media as validated information.

Comprehensive Physicochemical, Biocompatibility, and In Vivo Evaluation of a Nanofiber Gelatin Bone Graft Matrix for Bone Tissue Regeneration

Jason Sun
Duke University
Yu-Bin Huang
National Taiwan University
Yi-Chung Lai
National Taiwan University Hospital
Mei-Chun Yeh
Pojen General Hospital
Yi-Jie Kuo
Taipei Medical University - Hsin Kuo Min Hospital
Jui-Sheng Sun
drjssun@gmail.com

Landseed International Hospital
Zwei-Chieng Chang
National Taiwan University, National Taiwan University Hospital

Research Article

Keywords: biomaterials, bone regeneration, bone tissue engineering, large bone defects, nanofibers, nanotechnology

Posted Date: September 15th, 2026

DOI: https://doi.org/10.21203/rs.3.rs-10873970/v1

License: This work is licensed under a Creative Commons Attribution 4.0 International License.
Read Full License

Additional Declarations: No competing interests reported.

Version of Record: A version of this preprint was published at Journal of Orthopaedic Surgery and Research on November 3rd, 2026. See the published version at https://doi.org/10.1186/s13018-026-07348-4.

Abstract

Nanofiber-based biomaterials have emerged as promising bone tissue engineering scaffolds because they mimic the native extracellular matrix and promote bone regeneration. This study comprehensively evaluated the physicochemical properties, biocompatibility, and in vivo performance of a nanofiber gelatin bone graft matrix.

Material characterization included fiber morphology, crystallographic structure, phase composition, porosity, specific surface area, and tensile strength. Biological safety was assessed through qualitative and quantitative in vitro cytotoxicity assays, biocompatibility testing, subchronic systemic toxicity, and an in vitro mammalian cell gene mutation assay. Bone regeneration and local tissue responses were evaluated using a rabbit distal femoral implantation model at 1, 3, and 6 months.

The nanofiber gelatin matrix exhibited an average fiber diameter of 156.9 ± 26.0 nm, crystallinity of 97.3%, pore size of 182.4 ± 22.1 Å, specific surface area of 36.2 ± 2.5 m^2/g, porosity of 67.0 ± 1.6%, and tensile strength of 59.1 ± 4.6 N/mm^2. No evidence of in vitro cytotoxicity, systemic toxicity, or mutagenicity was observed. Histopathological evaluation demonstrated no adverse local tissue response over the 182-day implantation period (implantation score < 2.9). In vivo, the nanofiber gelatin bone graft matrix showed bone regeneration and degradation characteristics comparable to those of the predicate device, Socko Graftend Collagen Bone Graft.

These findings demonstrate that the nanofiber gelatinn bone graft matrix possesses favorable physicochemical properties, excellent biocompatibility, and effective bone regenerative performance, supporting its potential as a safe and effective scaffold for bone tissue engineering applications.

Key Highlights

- The nanofiber gelatin bone graft matrix demonstrated excellent physicochemical properties, mechanical strength, biocompatibility, and safety, with no cytotoxicity, systemic toxicity, mutagenicity, or adverse tissue reactions.
- In a rabbit model, it promoted effective bone regeneration comparable to a commercial collagen graft, highlighting its strong potential for bone tissue engineering and clinical applications.

1. Introduction

Age-related musculoskeletal disorders, including osteoporosis and osteoarthritis, together with trauma, tumor resection, and autoimmune diseases, are major causes of large bone defects and disability worldwide [1]. Although bone possesses an intrinsic capacity for regeneration, critical-sized defects exceed its natural healing potential and often require surgical intervention [2]. Conventional treatments, such as autografts and allografts, remain the clinical standard but are limited by donor-site morbidity, limited graft availability, risk of disease transmission, and immune rejection [3–5]. These limitations have

driven the development of bone tissue engineering (BTE) strategies that combine biomaterials with regenerative approaches to promote bone repair [6].

Nanotechnology has emerged as a promising approach in BTE because nanoparticles provide a high surface area, enhance mechanical properties, improve cell adhesion, proliferation, and osteogenic differentiation, and can impart antibacterial activity [7].

Among natural biomaterials, type I collagen and gelatin are widely used owing to their excellent biocompatibility, biodegradability, and osteoconductivity [8]. However, their relatively poor mechanical strength and rapid degradation limit their application as load-bearing scaffolds [9, 10].

Incorporation of bioactive ceramic nanoparticles, particularly hydroxyapatite (HA) and β-tricalcium phosphate (β-TCP), has been shown to enhance scaffold mechanical properties, osteo-conductivity, and bone regeneration both in vitro and in vivo [11–13]. In this study, a three-dimensional gelatin nanofiber scaffold coated with hydroxyapatite nanoparticles was developed to improve osteogenic performance. The scaffold was characterized for its physicochemical properties and evaluated for biocompatibility and in vivo bone regeneration.

The implantation study was conducted in accordance with **ISO 10993-6** and institutional standard operating procedures to evaluate the local tissue response to the hydroxyapatite-coated gelatin nanofiber scaffold following implantation in rat bone for 91 days. Tissue reactions were compared with those elicited by a control implant to assess the material's local biocompatibility and safety.

2. Materials and Methods

2.1.1 Fabrication of Nanofiber Gelatin Bone Graft Matrix

The nanofiber gelatin bone graft matrix was fabricated as previously described with some modification by mixing hydroxyapatite (10 g HA: < 200 nm in particle size; Sigma-Aldrich) within gelatin solution (Type A, porcine; Sigma-Aldrich) to the weight ratio of 1:1, cross-linked using 1% glutaraldehyde (Sigma-Aldrich), rinsed by dipping in ethanol (20 times), and then freeze-drying in 24 well plate [5].

2.1.2 Material Characterization

The nanofiber gelatin bone graft matrix was characterized for its morphology, crystallinity, thermal stability, porosity, specific surface area, and mechanical properties. Fiber morphology and diameter were examined by scanning electron microscopy (SEM; Hitachi TM-1000, Japan) in the range of 5–15 kV, and at 500x, 2000x, 5000x magnification for detailed observation; following gold sputter coating, and images were analyzed using MetaMorph software.

Crystalline structure and phase composition were determined by X-ray diffraction (XRD; Rigaku MiniFlex II) at the wavelength of 1.56 Å, 2θ scanning angle range to 20° to 60°, and the scanning speed to 0.02°/s; while thermal stability was evaluated by thermogravimetric analysis (TGA; PerkinElmer SDT600) under nitrogen from 30 to 1000°C at a rate of 10°C/min and hold for 5 minutes. Specific surface area and pore size distribution were measured by nitrogen adsorption using a surface area and pore size analyzer

(Micromeritics ASAP 2020), the flow rate was set at 30–50 mL/min and porosity was calculated from pore and total volumes. The obtained material weight, pore volume (Vp), and total volume (Vs) data are listed in **Supplementary Table 1**. The porosity of the material is then calculated using the porosity formula: $\emptyset$ = (Vp / Vp + Vs) × 100%.

Tensile strength was determined using a universal testing machine (Shimadzu AGS-X series) at a crosshead speed of 1 mm/min. The initial thickness, width, and maximum load data of the material are listed in **Supplementary Table 2**. The measured data were calculated using the formula:

Tensile Strength (MPa) = Maximum Load / Initial Cross-sectional Area of Sample (Thickness × Width).

2.2 In Vitro Cytotoxicity

Cytotoxicity was evaluated according to **ISO 10993-5** using L929 mouse fibroblasts (BCRC RM60091: Food Industry Research and Development Institute) cultured in α-MEM (HyClone, SH30568.01, AJ30760191) at 37 ± 1℃ in 5% CO_2 atmosphere. Test article extracts were prepared at a surface area-to-medium ratio of 3 cm²/mL by incubation at 37°C for 72 h. High-density polyethylene (HDPE) and 10% DMSO served as the negative and positive controls, respectively. Qualitative cytotoxicity was assessed by neutral red staining, the cells were scored by the change of cell morphology and viability under inverted microscope in accordance with criteria listed in **Supplementary Table 3;** the quantitative cell viability was determined using the MTT assay. The absorbance of test samples was represented as mean ± standard deviation (SD). Compared to the blank (as 100% viability), the percentage of viability and mortality was calculated by the following formula:

Viability (%) = (OD_{570e} / OD_{570b}) x 100%

Mortality (%) = 100 – Viability (%)

Where, OD_{570e} is the mean value of the measured absorbance of the test samples; OD_{570b} is the mean value of the measured absorbance of the blank (B). Cell viability ≥ 70% relative to the blank control was considered non-cytotoxic.

2.3 Biocompatibility Evaluation

Biocompatibility was assessed in accordance with the **ISO 10993** series. Genotoxicity was evaluated using the mouse peripheral blood micronucleus assay and the mouse lymphoma (L5178Y $TK^{+/-}$) gene mutation assay. The blood samples were smeared on acridine orange-coated slides and the presence of micronuclei in four thousand PCEs (polychromatic erythrocytes) was examined under fluorescent microscope (Zeiss AXIO Scope.A1) with 460–490 nm exciting and FITC long pass filter was used for polychromatic erythrocytes (PCE) and micronucleus counting.

Subchronic systemic toxicity was assessed following 13-week subcutaneous implantation in 40 Sprague-Dawley rats (20 male and 20 female) with evaluations including clinical observations, hematology, serum biochemistry, urinalysis, organ histopathology, and lesion severity grading. According

to the reference published in Toxicologic Pathology [14]. The criteria of severity grading system for all microscopic lesions were as follows: minimal (< 10%), mild (10–39%), moderate (40–79%), marked (80–100%).

2.3.1 Statistical analysis of histopathologic findings

In this study, the mentioned pathologic lesions of treatment group were recorded and compared to the same lesions in negative control group. The statistical analysis was performed by Microsoft Excel (2025) program for Windows®. Comparisons of histopathological grading parametric data collected from treatment and negative control groups performed by Student t test method. A p-value less than 0.05 was used as the criterion of significance.

2.4 In Vivo Study

All procedures were pre-approved and supervised under the Institutional Animal Care and Use Committee (IACUC) of the National Taiwan University College of Medicine and College of Public Health (Rat: Affidavit of Approval of Animal Use Protocol: #20230333) or the Institutional Animal Care and Use Committee of Master Laboratory Co., Ltd. in accordance with national animal welfare legislation (Rabbit: Affidavit of Approval of Animal Use Protocol: #25-PLAN-35). The study protocol and conformed to the National Institute of Health guidelines for the use of laboratory animals and all the procedures were performed in accordance with the ARRIVE guidelines.

For rats' experiment, 10-week-old male Wistar rats, weighing 200–250 g, were anesthetized with a 1:2 concentration of Zoletil (Virbac AH, Inc., Fort Worth, TX, USA) and Rompum (Bayer, Taipei, Taiwan) (1 mL/kg) via intraperitoneal injection. Local anesthesia (Articaine 40 mg, 1% epinephrine; Merck KGaA, Darmstadt, Germany) was performed at each surgical site for additional pain control and blood hemostasis; for rabbis' experiment, the New Zealand white rabbits (mean body weight, 3.0 ± 0.5 kg; age, 6 months) were procured from the Master Laboratory (Taiwan). All surgical procedures were performed under general anesthesia administered using an intramuscular injection of 15 mg/kg zoletil (Virbac Taiwan, Taipei, Taiwan) + 0.05 mL/kg rompun (Bayer Taiwan, Taipei, Taiwan). To induce analgesia, the rabbits were given 0.15 mg/kg oral meloxicam (Metacam; Boehringer Ingelheim Taiwan, Tai-wan) 1 day pre-operatively, immediately pre-operatively, and 2 days post-operatively. The euthanasia/sacrifice of animals were performed by an overdose of injectable anesthetics, such as pentobarbital, administered intravenously (rabbits) or intraperitoneally (rats).

2.4.1 Local Implantation Study

Local tissue response was evaluated according to **ISO 10993-6** using a rat femoral bone implantation model. Total of 12 male Wistar rats (10 weeks, Body weight > 120 g, BioLASCO Taiwan Co., Ltd.) were used in this study. A standardized 2.1 mm circular bone defect was created in each femur, with the test material implanted in one limb and high density polyethylene (HDPE) (USP, Lot No. K0M357) implanted contralaterally as the negative control. Animals were monitored for 182 days before histopathological

examination. Tissue reactions were scored according to ISO 10993-6, with an irritation score < 2.9 considered indicative of minimal or no local tissue reaction.

2.4.2 In Vivo Bone Regeneration

According to the review study of Kilborn et al. [15], bone regeneration was evaluated in a distal femoral defect model using skeletally mature New Zealand White rabbits (weight ≥ 2.8 kg and age ≥ 8 months). Total 36 skeletal matured New Zealand white rabbits were used, yielding 24 test article specimens, 24 predicate device specimens, and 24 sham specimens in this study. Cylindrical defects (6 mm × 10 mm) were implanted with either the Nanofiber gelatin Bone Graft Matrix or the predicate device (“Socko” Graftend Collagen Bone Graft, Lot. BDC001, New Taipei City, Taiwan), while untreated defects served as controls. Animals were euthanized at 1, 3, and 6 months post-implantation. Gross observations, radiographic examination, and histological analyses of undecalcified sections stained with Masson's trichrome were performed. Photographic images of the histological sections were taken to evaluate bone tissue and remaining implant material. New bone formation, residual bone substitute, and void space within each section were calculated and recorded for each animal. Bone tissue and remaining implant material were measured using the Media Cybernetics Image-Pro Plus (IPP) software (Rockville, Maryland US). The IPP system was spatially calibrated to ensure accurate determination of distance, area, and related parameters. The resulting datasets were exported and used for further statistical analysis. Histomorphometric analysis quantified new bone formation, residual graft material, and void area using Image-Pro Plus software.

3. Results

3.1 Material Characterization

SEM analysis revealed a uniform nanofibrous network with evenly distributed porous hydroxyapatite particles embedded within the fibers (Fig. 1A). The scaffold exhibited an average fiber diameter of **156.9 ± 26.0 nm**. XRD confirmed the characteristic hydroxyapatite crystalline phase with a major diffraction peak at approximately **32°**, corresponding to a high average crystallinity of **97.3%** (Fig. 1B). Thermogravimetric analysis showed an overall weight loss of approximately 30%, indicating that the scaffold consisted of approximately 30% organic (gelatin) and 70% inorganic (hydroxyapatite) components, with hydroxyapatite exhibiting excellent thermal stability (Fig. 1C).

Nitrogen adsorption analysis demonstrated an average pore size of 182.4 ± 22.1 Å, a specific surface area of 36.2 ± 2.5 m^2/g, and a porosity of 67.0 ± 1.6%. Mechanical testing showed an average tensile strength of 59.1 ± 4.6 N/mm^2 (Table 1).

Table 1
Experimental Results of Physical and chemical analysis (specific surface Area, pore size analysis and mechanical properties)

Specific Surface Area, Pore Size Analyzer						
	Pore Size (Å)	**BET Surface Area (m^2/g)**	**Weight (g)**	**Pore volume (Vp, cm^3/g)**	**Total volume (Vs, cm^3/g)**	**Porosity (%)**
Mean	182.394311	36.1971	0.2324	0.211	0.10324	67.036
Std Dev	22.1116181	2.446427211	0.016122965	0.0264	0.0071661	1.5592
Mechanical properties						
	Thickness (mm)	Width (mm)	Cross-sectional Area (mm^2)	Maximum Load (N)	Tensile Strength (N/mm^2)	
Mean	0.61	14.152	8.6871	513.35	59.04896	
Std Dev	0.1286468	1.995312006	2.460828629	159.29	4.5872239	
Note:						
The fibers were then carefully observed at 5000x magnification. Measurements and analysis revealed that the fiber diameter was 156.92 ± 26.04 nm which ranges from approximately 120 to 200 nm. (length 57–307 μm.)						

3.2 In Vitro Cytotoxicity

Qualitative neutral red staining showed normal spindle-shaped morphology of L929 fibroblasts following exposure to the scaffold extract, comparable to the blank and negative controls, whereas the positive control exhibited severe cytotoxicity (Fig. 2). Quantitative MTT analysis demonstrated cell viabilities of **71%** and **76%** for the undiluted and diluted extracts, respectively, exceeding the ISO 10993-5 cytotoxicity threshold of 70%. These results indicate that the nanofiber gelatin bone graft matrix is non-cytotoxic (**Supplementary Table 4**). The results of qualitative and quantitative assays showed “Zero” reactivity. Therefore, none in vitro cytotoxicity could be considered in the extract solution of the test Nano-fiber Gelatin Bone Graft Matrix.

3.3 Biocompatibility

The mouse peripheral blood micronucleus assay showed no increase in micronucleated polychromatic erythrocytes, indicating that the material did not induce chromosomal damage (**Supplementary Table 5**). In the 13-week rat implantation study, no treatment-related changes were observed in body weight, clinical signs, hematology, serum biochemistry, urinalysis, organ weights, or histopathology,

demonstrating the absence of subchronic systemic toxicity (**Supplementary Tables 6–8**). Similarly, the mouse lymphoma (L5178Y $TK^{+/-}$) assay demonstrated no significant increase in mutation frequency under any testing condition, confirming that the material was non-mutagenic (**Supplementary Table 8**).

3.4 Local Tissue Response

All rats survived the 182-day implantation period without complications. Gross examination revealed no evidence of inflammation, hemorrhage, necrosis, encapsulation, or foreign-body reaction. Histological evaluation according to ISO 10993-6 showed minimal residual material with normal tissue healing and an implantation score of 0.0, indicating no local tissue reaction compared with the HDPE control (Fig. 3; **Supplementary Tables 9–11**). Under the condition of this study, there were no specific adverse findings for 182 days observation. According to histopathological evaluation score as 0.0, indicate that the test Nano-fiber Geletin Bone Graft Matrix when implanted in bone for 182 days among SD rats, is considered as no reaction (Score < 2.9) to the tissue as compared to the negative control.

3.5 In Vivo Bone Regeneration

All rabbits recovered uneventfully, with normal weight gain and no postoperative complications (**Supplementary Tables 12–13**). Histomorphometric analysis demonstrated progressive bone regeneration in both the test and predicate device groups throughout the 6-month study (Fig. 4). The test scaffold degraded more gradually, with residual material observed at 3 and 6 months, whereas the predicate device was completely resorbed by 3 months. Despite these differences in degradation kinetics, no significant differences in new bone formation were observed between the two materials at any evaluation time point (**Supplementary Table 14**). Both materials supported comparable bone regeneration, although their relatively rapid degradation may have limited long-term space maintenance. Overall, the Nanofiber Gelatin Bone Graft Matrix demonstrated favorable physicochemical properties, excellent biocompatibility, absence of cytotoxicity, systemic toxicity, and mutagenicity, as well as a minimal local tissue response. Its in vivo bone regeneration performance was comparable to that of the predicate collagen bone graft while exhibiting a slower degradation profile.

4. Discussion

The treatment of critical-sized bone defects remains a major clinical challenge because conventional bone grafts, including autografts and allografts, are limited by donor-site morbidity, restricted availability, risk of disease transmission, and variable regenerative outcomes. Bone tissue engineering has therefore emerged as a promising strategy for developing biomimetic scaffolds that support bone regeneration [7]. Among these, nanostructured biomaterials have attracted considerable attention because they better replicate the nanoscale architecture of native bone extracellular matrix (ECM), thereby enhancing cell adhesion, proliferation, differentiation, and osteogenesis [7, 16, 17]. In the present study, the hydroxyapatite (HA)-coated gelatin nanofiber scaffold exhibited favorable physicochemical properties, including a highly porous nanofibrous architecture, high crystallinity, and adequate tensile strength [5, 18, 19]. These structural characteristics are desirable for bone regeneration because they facilitate cell

infiltration, nutrient transport, and mechanical stability while providing an osteoconductive environment. The high porosity and specific surface area are consistent with previous reports demonstrating that nanofibrous scaffolds promote osteoblast attachment and extracellular matrix deposition more effectively than conventional microscale scaffolds.

Typically, one of two types of polymers – natural or synthetic – is selected to be electrospun; the synthetic polymers, including polycaprolactone (PCL), poly(l-lactic acid) and poly(glycolic acid), among others, is quite flexible; but the biocompatibility of newly produced polymers must be carefully considered because these polymers lack bioactivity. On the other hand, many naturally occurring polymers, including gelatin, collagen, chitosan (CS) and silk, are frequently used to construct scaffolds, feature peptide sequences that influence cell proliferation, adhesion and differentiation as part of their inherent bioactivity [20]. Electrospinning may enhance the surface alignment, degree of porosity and structure of nanofibers. Electrospinning can enhance cellular viability and infiltration by mimicking the hierarchical ECM architecture by processing multiple polymeric materials and manipulating cellular behaviors for regenerative medicine [21, 22]. The biological evaluation further demonstrated the excellent safety profile of the scaffold. No evidence of cytotoxicity, genotoxicity, mutagenicity, subchronic systemic toxicity, or adverse local tissue reactions was observed, confirming its biocompatibility in accordance with the ISO 10993 series. These findings support previous studies showing that gelatin and hydroxyapatite are highly biocompatible materials for bone tissue engineering and that nanoscale surface features can enhance cellular responses without compromising biological safety.

In the rabbit femoral defect model, the HA-coated gelatin nanofiber scaffold supported bone regeneration comparable to that of the predicate collagen bone graft. Although the scaffold exhibited a slower degradation profile than the control material, both materials demonstrated similar levels of new bone formation throughout the study. A more gradual degradation may provide prolonged structural support during early bone healing; however, the relatively rapid resorption of both materials compared with the rate of bone formation suggests that further optimization of degradation kinetics may improve long-term defect bridging and space maintenance [23].

The favorable performance of the scaffold can be attributed to the synergistic combination of gelatin nanofibers and hydroxyapatite nanoparticles [24]. Gelatin provides a biomimetic extracellular matrix that promotes cell attachment and migration, whereas hydroxyapatite enhances osteoconductivity, mechanical strength, and mineralization [25]. Similar nanocomposite scaffolds have consistently demonstrated improved osteogenic performance compared with conventional collagen- or polymer-based scaffolds, highlighting the importance of mimicking the hierarchical structure of native bone [26].

Despite these encouraging findings, several limitations should be acknowledged. This study has several limitations. First, the scaffold was evaluated only in small-animal models; although the rat and rabbit models are well established for assessing biocompatibility and bone regeneration, they do not fully replicate the biological and mechanical environment of human bone. Second, only a single scaffold

formulation was investigated, and the influence of hydroxyapatite content, pore architecture, fiber diameter, and degradation rate on osteogenesis was not examined. Third, bone regeneration was assessed primarily by histological and histomorphometric analyses. Additional evaluations, such as micro-computed tomography (micro-CT), biomechanical testing, and quantitative molecular analyses of osteogenic and angiogenic markers, would provide a more comprehensive assessment of scaffold performance. Finally, although the scaffold demonstrated excellent safety and biocompatibility, the observation period was limited to six months, and long-term remodeling, functional integration, and clinical performance remain to be determined. Future studies should optimize scaffold composition and degradation rate, investigate the incorporation of osteogenic or angiogenic bioactive molecules, and evaluate patient-specific scaffold fabrication using advanced manufacturing technologies such as three-dimensional (3D) printing [27, 28]. Combining nanotechnology with additive manufacturing offers the potential to fabricate customized scaffolds with controlled pore architecture, improved mechanical properties, and spatiotemporal delivery of biological cues, thereby facilitating clinical translation. Validation in large-animal models and well-designed clinical studies will be essential for successful clinical translation.

Overall, the HA-coated gelatin nanofiber scaffold demonstrated excellent physicochemical characteristics, biocompatibility, and in vivo bone regenerative performance comparable to a commercially available collagen bone graft. These findings support its potential as a safe and effective biomaterial for bone tissue engineering and warrant further investigation in large-animal studies and clinical applications.

5. Conclusion

The present study demonstrated that the hydroxyapatite-coated gelatin nanofiber bone graft matrix possesses favorable physicochemical characteristics, including a highly porous nanofibrous architecture, high crystallinity, and adequate mechanical strength. Comprehensive biological evaluation confirmed excellent biocompatibility, with no evidence of cytotoxicity, genotoxicity, mutagenicity, subchronic systemic toxicity, or adverse local tissue reactions in accordance with ISO 10993 standards. In a rabbit femoral defect model, the scaffold supported bone regeneration comparable to that of a commercially available collagen bone graft while exhibiting a slower degradation profile that may provide prolonged structural support during early healing.

Collectively, these findings demonstrate that the hydroxyapatite-coated gelatin nanofiber scaffold is a safe and promising biomaterial for bone tissue engineering. Its biomimetic nanostructure, favorable biological performance, and regenerative capability support its potential as an alternative bone graft substitute for the treatment of critical-sized bone defects. Further optimization and validation in large-animal models and clinical trials are warranted to facilitate its translation into clinical practice.

Declarations

Conflict of interest statement: The authors declare no conflict of interest.

Acknowledgments: The authors would like to express their immense gratitude to LEON Biotech. Co., Ltd. (Kaohsiung, Taiwan), BioLASCO Taiwan Co., Ltd. (New Taipei City, Taiwan), and Mater Laboratory Co., Ltd. (Taipei, Taiwan) for their technical support. We also thank the Sheng Chen International Biomedical Corporation, Ltd, (Taiwan, ROC) for their kindness of providing the prescription or recipe of their product.

Consent for publication: Not applicable.

Availability of data and material: The datasets used and/or analyzed in the current study are available from the corresponding author on reasonable request.

Funding: This work was supported by the National Science and Technology Council, Taipei, Taiwan, ROC [NSTC 115-2314-B-002-093 & NSTC 115-2314-B-706-001].

Commercial Associations:

Yi-Chung Lai, Yi-Jie Kuo and Jui-Sheng Sun are co-funders of Sheng Chen International Biomedical Corporation, Ltd, (Taiwan, ROC).

Other authors certify that they have no commercial associations (e.g., consultancies, stock ownership, equity interest, patent/licensing arrangements, etc.) that might pose a conflict of interest in connection with the submitted article.

Location of work: All work was conducted at National Taiwan University, National Taiwan University Hospital (Taipei City, Taiwan).

Author Contributions:

Jason SUN and **Yu-Bin Huang**: Assistance with study conceptualization and design, Data collection, data analysis, and manuscript drafting.

Yi-Chung Lai and **Chih-Hsiang Fang**: Active discussion of experimental design, data collection, performing part of the experimental study and assembly.

Yi-Jie Kuo: Active discussion of experimental design,

Jui-Sheng Sun and **Jenny Zwei-Chieng Chang**: Study supervision, assistance with study conceptualization and design, analysis and interpretation of data, critical revision of the article for important intellectual content.

All authors have read and approved the final submitted manuscript.

References

1. Wu Y, Ji Y, Lyu Z. 3D printing technology and its combination with nanotechnology in bone tissue engineering. Biomed Eng Lett. 2024;14(3):451–64.
2. Keating JF, Simpson AH, Robinson CM. The management of fractures with bone loss. J Bone Joint Surg Br. 2005;87(2):142–50.
3. Collaborators GF. Global, regional, and national burden of bone fractures in 204 countries and territories, 1990–2019: a systematic analysis from the Global Burden of Disease Study 2019. Lancet Healthy Longev. 2021;2(9):e580–92.
4. Sözen T, Özışık L, Başaran N. An overview and management of osteoporosis. Eur J Rheumatol. 2017;4(1):46–56.
5. Fang CH, Sun CK, Lin YW, Hung MC, Lin HY, Li CH, Lin IP, Chang HC, Sun JS, Chang JZ. Metformin-Incorporated Gelatin/Nano-Hydroxyapatite Scaffolds Promotes Bone Regeneration in Critical Size Rat Alveolar Bone Defect Model. Int J Mol Sci 23(1) (2022).
6. Delpierre A, Savard G, Renaud M, Rochefort GY. Tissue Engineering Strategies Applied in Bone Regeneration and Bone Repair. Bioeng (Basel) 10(6) (2023).
7. Bauso LV, La Fauci V, Longo C, Calabrese G. Bone Tissue Engineering and Nanotechnology: A Promising Combination for Bone Regeneration. Biology (Basel) 13(4) (2024).
8. Fan L, Ren Y, Emmert S, Vučković I, Stojanovic S, Najman S, Schnettler R, Barbeck M, Schenke-Layland K, Xiong X. The Use of Collagen-Based Materials in Bone Tissue Engineering. Int J Mol Sci 24(4) (2023).
9. Liu S, Sun Y, Fu Y, Chang D, Fu C, Wang G, Liu Y, Tay FR, Zhou Y. Bioinspired Collagen-Apatite Nanocomposites for Bone Regeneration. J Endod. 2016;42(8):1226–32.
10. Loyo C, Cordoba A, Palza H, Canales D, Melo F, Vivanco JF, Baier RV, Millán C, Corrales T, Zapata PA. Effect of Gelatin Coating and GO Incorporation on the Properties and Degradability of Electrospun PCL Scaffolds for Bone Tissue Regeneration. Polym (Basel) 16(1) (2023).
11. D'Amora U, Ronca A, Scialla S, Soriente A, Manini P, Phua JW, Ottenheim C, Pezzella A, Calabrese G, Raucci MG, Ambrosio L. Bioactive Composite Methacrylated Gellan Gum for 3D-Printed Bone Tissue-Engineered Scaffolds. Nanomaterials (Basel) 13(4) (2023).
12. Murakami S, Miyaji H, Nishida E, Kawamoto K, Miyata S, Takita H, Akasaka T, Fugetsu B, Iwanaga T, Hongo H, Amizuka N, Sugaya T, Kawanami M. Dose effects of beta-tricalcium phosphate nanoparticles on biocompatibility and bone conductive ability of three-dimensional collagen scaffolds. Dent Mater J. 2017;36(5):573–83.
13. Jing T, Yi L, Xu L, Chen C, Liu F. The incorporation of β-tricalcium phosphate nanoparticles within silk fibroin composite scaffolds for enhanced bone regeneration: An in vitro and in vivo study. J Biomater Appl. 2022;36(9):1567–78.
14. Shackelford C, Long G, Wolf J, Okerberg C, Herbert R. Qualitative and quantitative analysis of nonneoplastic lesions in toxicology studies. Toxicol Pathol. 2002;30(1):93–6.
15. Kilborn SH, Trudel G, Uhthoff H. Review of growth plate closure compared with age at sexual maturity and lifespan in laboratory animals. Contemp Top Lab Anim Sci. 2002;41(5):21–6.

16. Hajiali H, Ouyang L, Llopis-Hernandez V, Dobre O, Rose F. Review of emerging nanotechnology in bone regeneration: progress, challenges, and perspectives. Nanoscale. 2021;13(23):10266–80.
17. Liang W, Zhou C, Bai J, Zhang H, Long H, Jiang B, Liu L, Xia L, Jiang C, Zhang H, Zhao J. Nanotechnology-based bone regeneration in orthopedics: a review of recent trends. Nanomed (Lond). 2024;19(3):255–75.
18. Lenne PF, Trivedi V. Sculpting tissues by phase transitions. Nat Commun. 2022;13(1):664.
19. Sun CK, Weng PW, Chang JZ, Lin YW, Tsuang FY, Lin FH, Tsai TH, Sun JS. Metformin-Incorporated Gelatin/Hydroxyapatite Nanofiber Scaffold for Bone Regeneration. Tissue Eng Part A. 2022;28(1–2):1–12.
20. Cheng X, Liu YT, Si Y, Yu J, Ding B. Direct synthesis of highly stretchable ceramic nanofibrous aerogels via 3D reaction electrospinning. Nat Commun. 2022;13(1):2637.
21. Dhand C, Ong ST, Dwivedi N, Diaz SM, Venugopal JR, Navaneethan B, Fazil MH, Liu S, Seitz V, Wintermantel E, Beuerman RW, Ramakrishna S, Verma NK, Lakshminarayanan R. Bio-inspired in situ crosslinking and mineralization of electrospun collagen scaffolds for bone tissue engineering. Biomaterials. 2016;104:323–38.
22. Yao Q, Cosme JG, Xu T, Miszuk JM, Picciani PH, Fong H, Sun H. Three dimensional electrospun PCL/PLA blend nanofibrous scaffolds with significantly improved stem cells osteogenic differentiation and cranial bone formation. Biomaterials. 2017;115:115–27.
23. Walsh WR, Oliver RA, Pelletier MH, Wang T, Christou C, Walsh ER, Page JM, Davis CT, Williams GM. Comparative Performance of Calcium Phosphate Grafts and Iliac Crest Autograft in Posterolateral Spinal Fusion in Rabbits. JOR Spine. 2025;8(3):e70101.
24. Ma K, Liao C, Huang L, Liang R, Zhao J, Zheng L, Su W. Electrospun PCL/MoS(2) Nanofiber Membranes Combined with NIR-Triggered Photothermal Therapy to Accelerate Bone Regeneration. Small. 2021;17(51):e2104747.
25. Ye G, Bao F, Zhang X, Song Z, Liao Y, Fei Y, Bunpetch V, Heng BC, Shen W, Liu H, Zhou J, Ouyang H. Nanomaterial-based scaffolds for bone tissue engineering and regeneration. Nanomed (Lond). 2020;15(20):1995–2017.
26. Di Pompo G, Liguori A, Carlini M, Avnet S, Boi M, Baldini N, Focarete ML, Bianchi M, Gualandi C, Graziani G. Electrospun fibers coated with nanostructured biomimetic hydroxyapatite: A new platform for regeneration at the bone interfaces. Biomater Adv. 2023;144:213231.
27. Kumar S, Nehra M, Kedia D, Dilbaghi N, Tankeshwar K, Kim KH. Nanotechnology-based biomaterials for orthopaedic applications: Recent advances and future prospects. Mater Sci Eng C Mater Biol Appl. 2020;106:110154.
28. Kim M, Wang X, Li Y, Lin Z, Collins CP, Liu Y, Ahn Y, Tsal HM, Song JW, Duan C, Zhu Y, Sun C, He TC, Luo Y, Reid RR, Ameer GA. Personalized composite scaffolds for accelerated cell- and growth factor-free craniofacial bone regeneration. Bioact Mater. 2024;41:427–39.

Figures

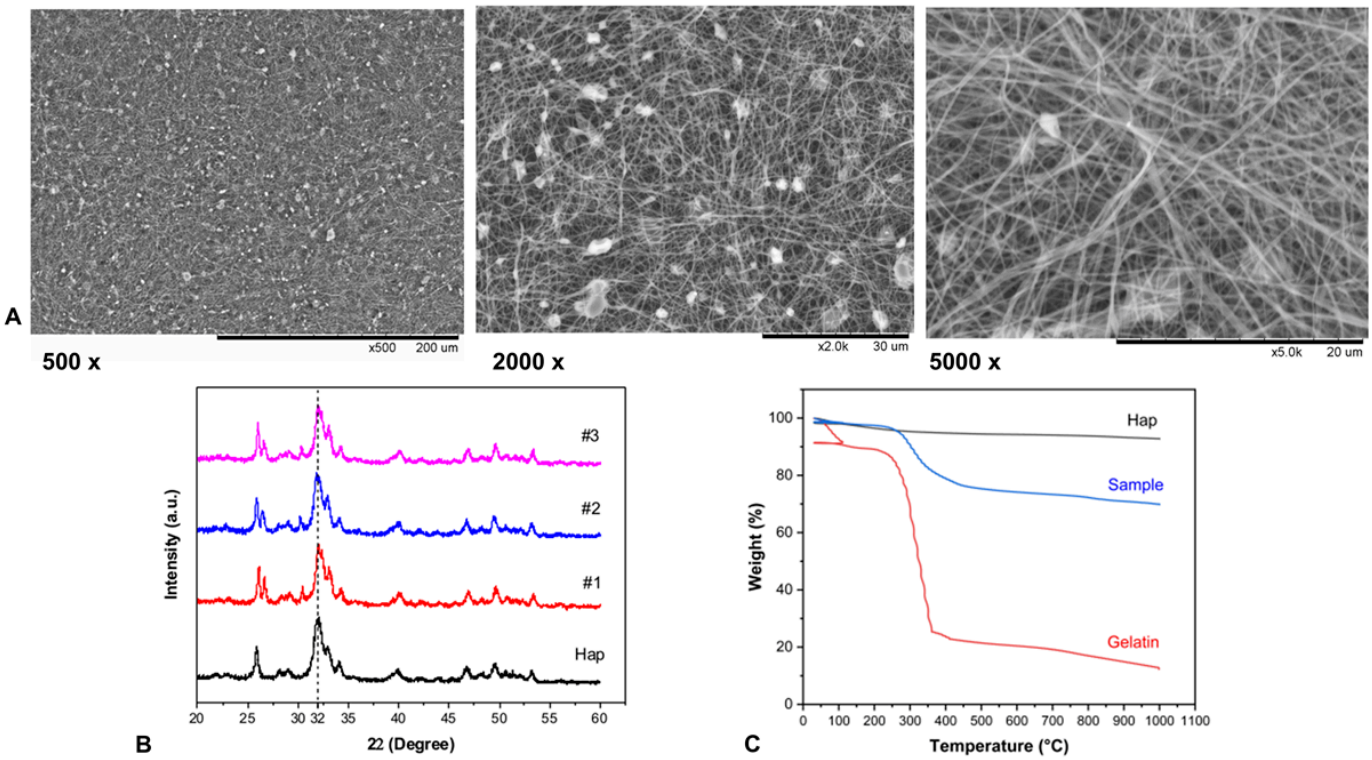


Figure 1

Material Fiber Testing and Analysis

A. Electron microscopy observation at 500-2000-5000x magnification

B. X-ray diffraction analysis: Compare this characteristic peak with the thermo-derived hydroxyapatite standard to determine if the peak intensity and position match.

C. Thermogravimetric analysis: Figure shows the thermogravimetric analysis (TGA) curve. The three curves represent: black line – inorganic standard (hydroxyapatite, Hap); blue line – nanofiber artificial bone material (Sample); and red line – organic standard (gelatin) – weight loss at different temperatures.

The weight of the nanofiber artificial bone material decreased from 100% to about 70%, with an overall thermogravimetric loss of 30%, indicating that the organic components accounted for 30% of the total weight of the sample, while the inorganic components accounted for 70%.

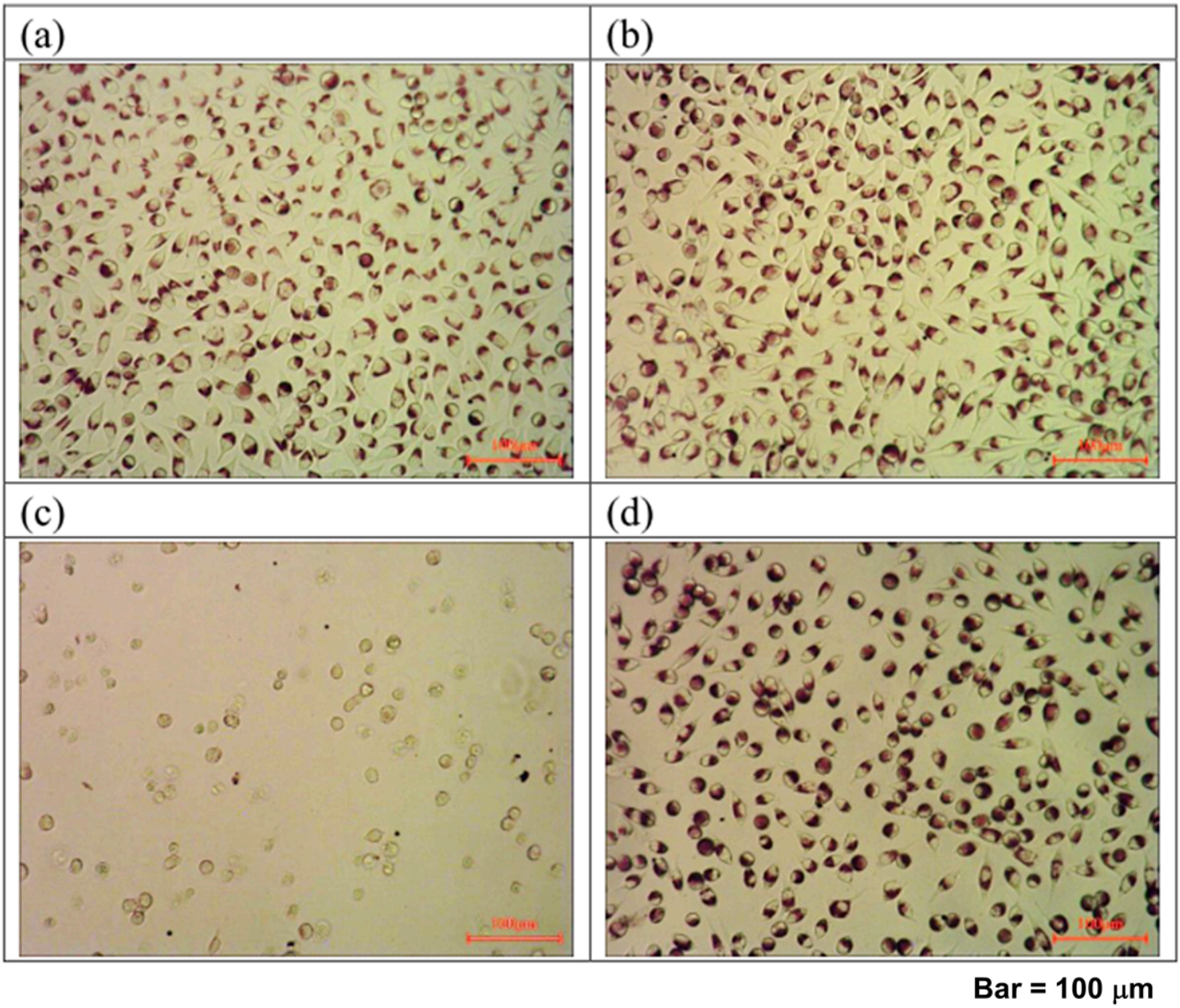


Figure 2

Supplementary-In vitro cytotoxicity test

The observed cell morphology of L929 cells after being treated for 24h under 100X inverted microscope.

a. Blank (B): culture medium

b. Negative control (NC): HDPE (High-density polyethylene)

c. Positive control (PC): 10% DMSO (Dimethyl sulfoxide)

d. Test article group: Nano-fiber Gelatin Bone Graft Matrix

Bar = 100 mm

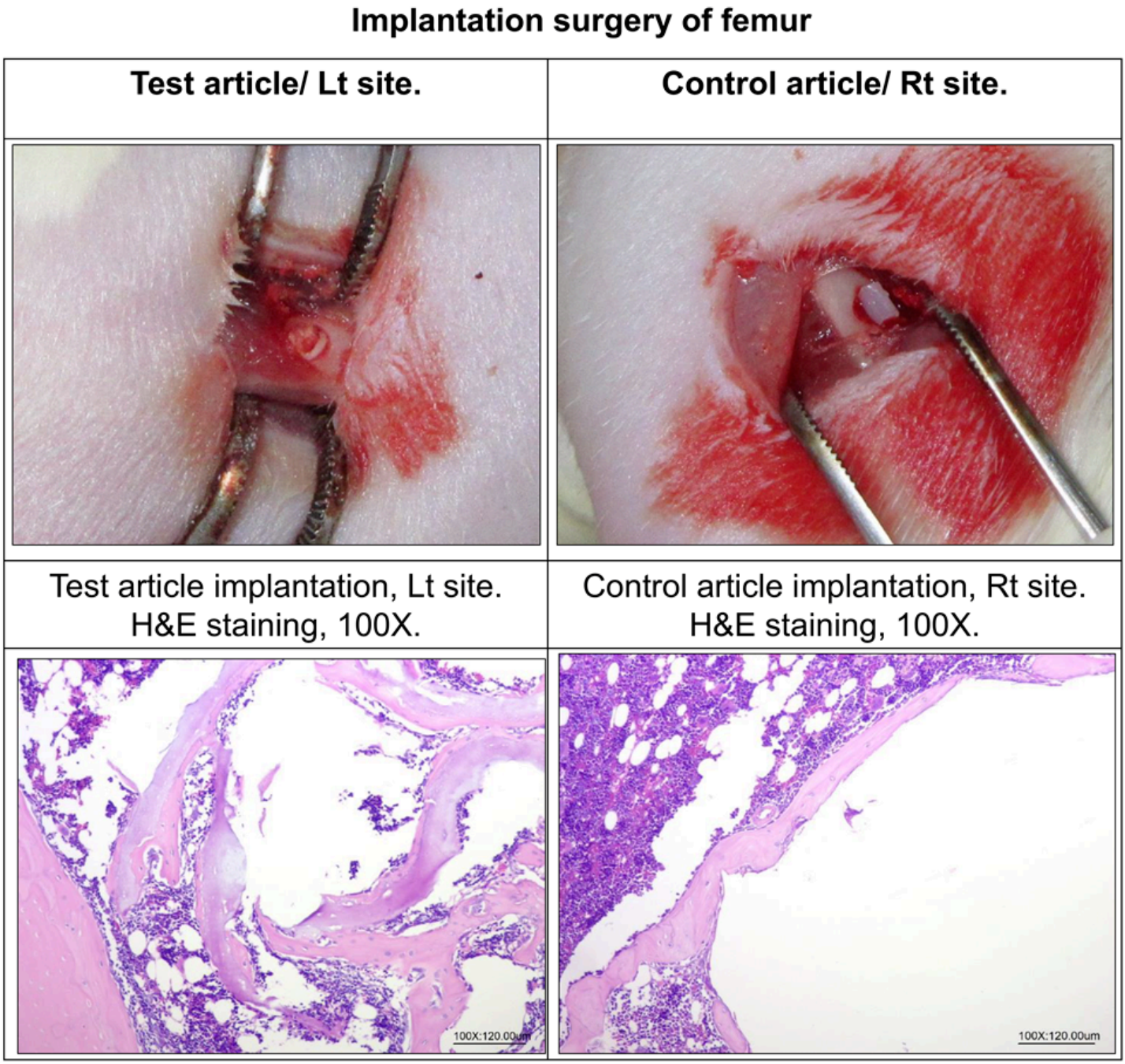


Figure 3

Histopathological evaluations

The general histopathological evaluation of the implantation sites, the score of 0.0 in 182 days, inferred that the test article showed no reaction after 182 days implantation.

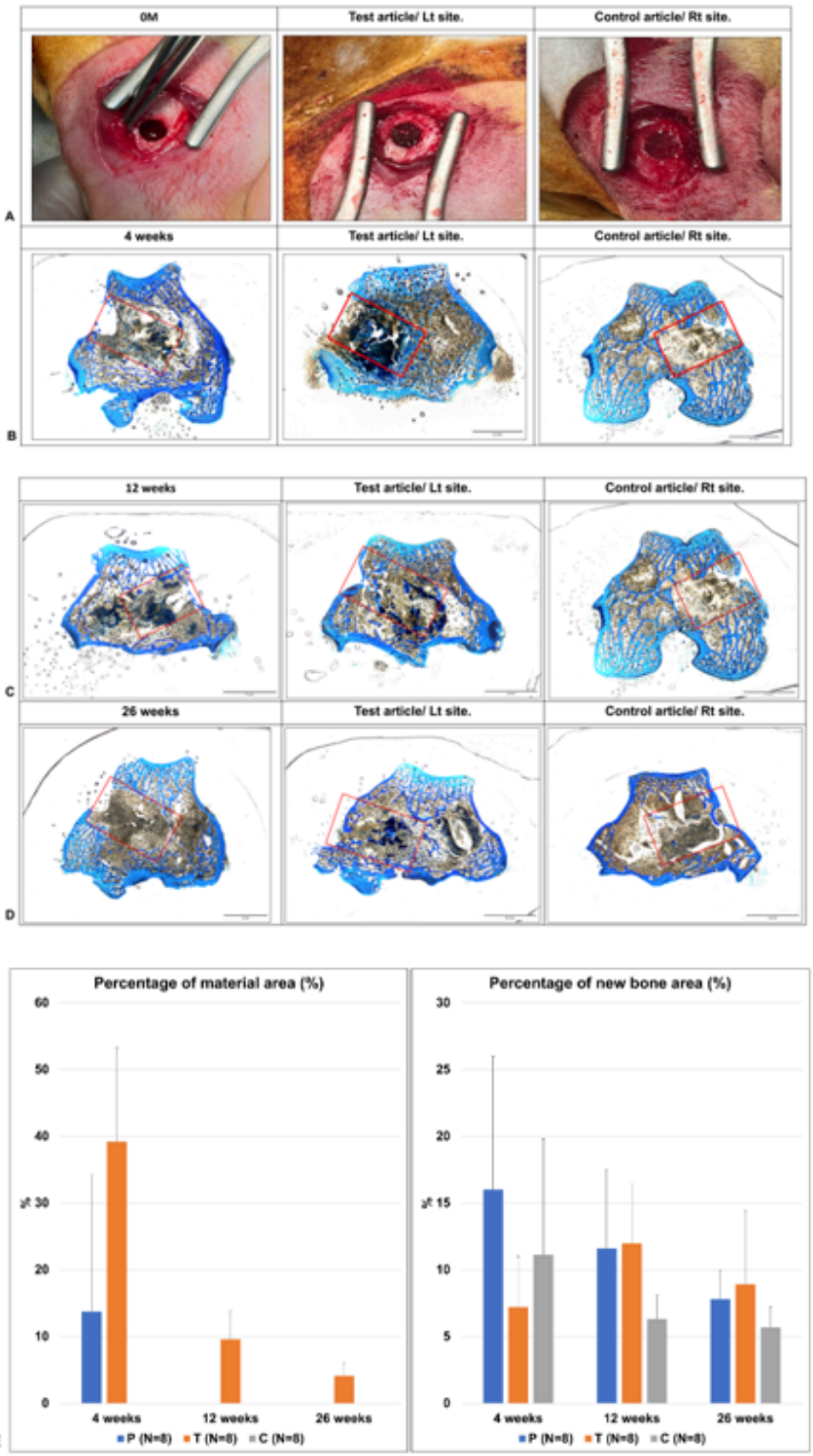


Figure 4

Histomorphomtetric evaluation of performance.

A. 0 week, B. 4 weeks, C. 12 weeks, D: 26 weeks, E: Histomorphomtetric Measurements.

Bar = 5 mm.

Supplementary Files

This is a list of supplementary files associated with this preprint. Click to download.

- Suppl202608BoneGraftJOSR.docx